Solid-state Raman laser generating discretely tunable ultraviolet between 266 and 320 nm

Richard P. Mildren, Hamish Ogilvy, and James A. Piper

Centre for Lasers and Applications, Macquarie University, Sydney, New South Wales 2109, Australia

Received November 2, 2006; revised January 8, 2007; accepted January 8, 2007;
posted January 12, 2007 (Doc. ID 76709); published March 5, 2007

We report a $KGd(WO_4)_2$ Raman laser pumped by a 532 nm laser that uses the intracavity nonlinear second harmonic and sum-frequency mixing of the Stokes and fundamental fields in β-barium borate to generate selectable output among eight output wavelengths over the range 266–320 nm. Output pulse energies of up to 0.22 mJ at 10 Hz pulse repetition rate and average output powers up to 48 mW at 5 kHz were achieved.

OCIS codes: 140.3550, 190.5650.

Few UV lasers sources exist at wavelengths between the third and fourth harmonics of Nd lasers (265–350 nm), a spectral region where there is emerging demand in biohazard detection, environmental sensing, and defense. Cerium-doped fluoride lasers[1] and AlGaN semiconductor diodes[2] are currently receiving substantial interest owing to their significant practical advantages over frequency-doubled dye lasers and optical parametric oscillators. There is a need, however, for robust narrowband sources with a broad tuning range.

Solid-state Raman lasers are versatile sources of laser output in the mid-IR and yellow-orange regions of the spectrum.[3] The resonator designs are varied from simple external-cavity wavelength converters,[4] compact self-Raman lasers,[5] and wavelength agile Raman lasers.[6,7] Conversion efficiencies for the Raman process often exceed 50% and in some cases approach the quantum limit.[8,9] While direct nonlinear frequency conversion of visible (e.g., yellow) Raman lasers provides a straightforward method of generating UV output near 290 nm,[10] important advantages are to be gained by placing the sum-frequency (SF) or second-harmonic (SH) medium intracavity. The higher intracavity fields in the nonlinear medium assist in enhancing conversion efficiency. Also, for resonators designed to co-oscillate fundamental and multiple Stokes fields, output at a range of SFs or SHs may be selected according to the phase-matching conditions in the nonlinear crystal. For example, switchable output among four laser wavelengths in the range 532–606 nm has been demonstrated for an intracavity Raman laser by angle tuning or temperature tuning an intracavity lithium borate SF medium.[6]

Here we report a solid-state UV Raman laser pumped at 532 nm that utilizes intracavity Raman and intracavity SF mixing to generate wavelength-switchable UV output at wavelengths that span the entire UV-B (i.e., 280–315 nm) as well as extending slightly into the neighboring UV-A (315–400 nm) and UV-C (200–280 nm) regions. We have characterized the laser performance for two pump lasers, a 10 Hz source for investigation of high output pulse energy generation and a 5 kHz source for investigation of performance at the higher pulse rates and average powers demanded by many applications in biological and environmental sensing.

The Raman laser consisted of a $KGd(WO_4)_2$ (KGW) Raman crystal and β-barium borate (BBO) nonlinear mixing medium positioned in a resonator as shown in Fig. 1. The input coupler is highly transmissive (~90%) at 532 nm and highly reflective for the first three Stokes orders (559–660 nm). The KGW crystal (5 mm × 5 mm × 50 mm), was antireflection coated for 532–600 nm and oriented to access the highest-gain Stokes shift of KGW at 901 cm^{-1} (i.e., laser propagation along the N_g crystallo-optic axis and pump polarization parallel to N_m). The SH or SFs of the intracavity Stokes and fundamental fields were coupled from the resonator by using a UV reflecting dichroic mirror (BSR-25-1025, CVI Laser LLC) placed between the BBO crystal (dimensions 4 mm × 4 mm × 7 mm, cut angle 44°) and the Raman crystal. This method of output coupling ensures that generated UV does not impinge on the KGW crystal, which has poor transmission for $\lambda < 350$ nm.

Both pump lasers were frequency-doubled, electro-optic Q-switched, Nd:YAG lasers of pulse duration typically 10 ns full width at half-maximum. The 10 Hz pump laser was a commercial flashlamp-pumped system (Lumonics, HyperYag), and the 5 kHz system was an air-cooled diode-pumped laser of the type described in Ref. 11. Imaging optics were used to provide good overlap between the pump and the Raman laser modes in the Raman crystal (~500 μm at 10 Hz and ~75 μm at 5 kHz). At 10 Hz, the input beam diameter was ~0.5 mm, and the radius of curvature of the input coupler and end mirrors were 100 and 200 cm, respectively. For the 5 kHz

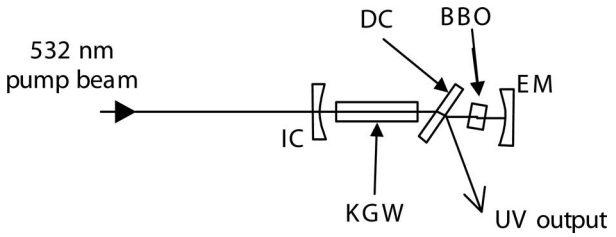

Fig. 1. Schematic diagram of the UV Raman laser. IC, input coupler; DC, dichroic mirror; EM, end mirror; BBO, β-barium borate crystal.

0146-9592/07/070814-3/$15.00

pump source, the pump laser was focused into the resonator by using a 100 mm lens, and the curvatures of the input coupler and end mirror were 20 and 30 cm, respectively.

The UV output pulses were separated from residual visible output by using a Pellin–Broca prism. The quoted pump powers and efficiencies are based on the measured pump power incident on the input mirror. The output wavelength was measured using a fiber-coupled spectrometer (USB2000, Ocean Optics). Temporal pulse shapes of the UV and residual visible Stokes orders were recorded on storage oscilloscope (500 MHz TDS3054, Tektronix) by first dispersing the output beam with a 600 line/mm grating and illuminating the selected order onto a fast-response silicon photodiode (Thorlabs DET2-SI).

The output wavelength was selected by rotating the BBO nonlinear mixing crystal in the horizontal plane. Though a change in wavelength can easily be achieved without realignment of the end mirror, alignment was reoptimized upon each wavelength change to generate maximum output. For the 10 Hz pump laser, the UV output for each of the eight wavelengths varied with input pulse energy as shown in Fig. 2. The pulse energy at the SH of the pump wavelength (266 nm) increased to 130 μJ at more than 5% conversion efficiency but saturated for higher input energy. The saturation coincides with the onset of significant Stokes generation, indicating that the 266 nm output is limited by pump depletion from the competing Raman process.

Rotating the angle of the BBO crystal by $\sim 3°$ (in the direction that decreases the subtended angle between the beam and optical axes) steps the output wavelength 273 nm, corresponding to the SF of the fundamental and the first Stokes. As with many of the UV wavelengths, the threshold is approximately 1–2 mJ, the output pulse energy increases monotonically over the investigated range of input energy, and the slope efficiency diminishes for input pulse energies >4 mJ. The peak 273 nm conversion efficiency was 1.35% from 4.5 mJ input energy, while the maximum output pulse energy achieved was 104 μJ at conversion efficiency 0.75%.

Generation of 279 nm output, the SH of the first Stokes, increases with pump energy in a way similar to that observed for 273 nm but is approximately twice as efficient. The maximum output energy was 223 μJ (i.e., 2.2 mW of average output power) at 1.5% conversion efficiency from the pump. The maximum conversion efficiency was 2.4% obtained at ~ 4 mJ input energy. We have found that the conversion efficiencies for SHs are often notably higher than neighboring SF wavelengths for both pump lasers. A summary of the output wavelengths, the maximum energies, and conversion efficiencies achieved are summarized in Table 1. For example, the conversion efficiency of 287 nm (the SF of the first and second Stokes) is very similar to 273 nm, whereas output at 295 nm (the SH of the second Stokes) is similar to 279 nm. Though we have yet to investigate this fully, preliminary measurements of temporal pulse shapes indicate that the SF conversion efficiencies are typically lower at least in part because of reduced temporal overlap of the subharmonic components in the BBO crystal. For the longer wavelengths corresponding to nonlinear mixing of third and fourth Stokes, efficiency is primarily limited by the UV bandwidth of the resonator mirrors (refer also to Table 1). For example, for SH output of the third Stokes (311 nm), the lower output efficiency (1.1%) compared with the shorter-wavelength SHs can be attributed to substantial loss at the end mirror, measured to be $\sim 35\%$ at 311 nm. For 320 nm, the efficiency is $<0.1\%$ owing to significant losses at both the end mirror (65%) and the output coupler ($\sim 10\%$).

An analysis of the factors that influence conversion efficiency at each wavelength would require consideration of the competing nonlinear SF and Raman cascading processes as well as the resonator losses at each wavelength. However, the qualitative features of the observed behavior are consistent with the expected energy transfer among the Stokes orders. The decrease in slope efficiency of wavelengths 273–294 nm for pump energies above 4 mJ is consistent with depletion of the harmonic components by the cascade of energy to higher Stokes orders. By displaying the dispersed output on a screen, we clearly observed four Stokes orders when the BBO crystal was angled at phase matching and also when inclined slightly to inhibit UV generation. Though the intensities of the higher Stokes orders were reduced when the BBO was tuned for generating efficient UV output, it is deduced that the Raman process is in close competition with nonlinear SF generation. In contrast, the effect of such cascading on generation of UV output >300 nm (corresponding to SF generation or SH generation of the third or fourth Stokes wavelengths) is reduced, since the threshold for cascading to higher Stokes is raised by increased resonator losses. This is consistent with the more linear output-versus-input energy behavior observed for wavelengths ≥ 302 nm.

For the 5 kHz pump source, the output powers and efficiencies obtained as a function of wavelength are shown in Table 2. The maximum output of 47 mW was obtained for 279 nm at 2.7% conversion effi-

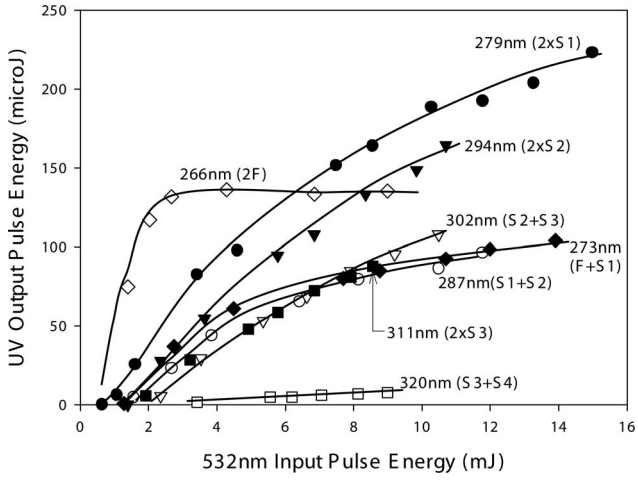

Fig. 2. Output versus input energy at 10 Hz for each UV wavelength (F, fundamental; S, nth Stokes).

Table 1. UV Wavelength, Output Energy, and Efficiency Obtained at 10 Hz

Output Wavelength (nm)	Wavelength Assignment[a]	Max Energy (μJ)	Max Efficiency (%)	End-Mirror Reflectance (%)	Dichroic Reflectance (%)
266.0	SHG F	136	5.8	>99	98.5
272.6	SFG F+S1	104	1.4	>99	>99
279.4	SHG S1	223	2.4	>99	>99
286.7	SFGS1+S2	96	1.1	>99	>99
294.4	SHG S2	164	1.6	>99	>99
302.3	SFGS2+S3	108	1.1	>99	>99
310.8	SHG S3	88	1.1	71.5	98
319.7	SFGS3+S4	7.7	0.1	29	95

[a]Note that UV output may be derived by SF generation (SFG) of Stokes wavelengths separated by two or more orders; however, the corresponding phase matching angles are slightly displaced from the angle at which maximum output is obtained. SHG, second-harmonic generation.

Table 2. Maximum Output Power and Efficiency for the 5 kHz Pump Source

Wavelength (nm)	Output power (mW)	Max. Efficiency (%)
266.0	40	3.2
272.6	11	0.85
279.4	47	2.7
286.7	17	0.90
294.4	25	1.4
302.3	1.5	0.08

ciency. Output for wavelengths >302 nm was not obtained because of the narrower bandwidth of the mirrors used in this arrangement. The maximum conversion efficiencies for many of the wavelengths are similar to those obtained at 10 Hz, and again the SH wavelengths are approximately twice as efficient as the SFs, except for wavelengths >295 nm, for which resonator losses affect the conversion efficiency more strongly. Evidence of thermal lensing in the Raman medium is not observed at the current pump levels (see also Ref. 9).

There is substantial scope to extend the performance of the 532 nm pumped UV Raman lasers detailed above. It should be noted that output wavelengths and tuning range depend on the selected optics and may vary significantly from the two examples of this Letter. As mentioned above, the wavelength spacing can be reduced from 901 to 768 cm^{-1} by rotating the KGW 90° about the propagation axis. It may also be useful to use Raman materials having a different Stokes shift to target specific output wavelengths. Though the tuning range demonstrated above is already large, the accessible wavelength range may also be extended to longer wavelengths by using mirrors of increased bandwidth.

Note that very little attempt was made to optimize waist sizes, crystal material and length, cavity optics, and thus greater efficiencies are anticipated. The results above also show that the efficiency for many output wavelengths is limited by competition between the nonlinear mixing process and further Raman conversion to higher Stokes orders. Conversion efficiency may thus be improved by increasing the nonlinear coupling coefficient for harmonic mixing, which could be achieved in practice, for example, by paying additional attention to the beam properties through the BBO crystal to ensure that propagation is within the narrow acceptance angle of BBO. Cylindrical focusing geometries, used successfully to improve conversion efficiency in BBO, may also be applied in this case by the use of anamorphic resonator optics. Power loss by cascading to higher Stokes may also be reduced or eliminated by introducing resonator losses at the higher Stokes order by, for example, careful selection of coatings (though such an approach is most applicable to boosting efficiency at a selected wavelength). By addressing these issues, we believe that widely tunable UV Raman lasers are likely to be realized with conversion efficiencies higher than 10%.

The authors gratefully acknowledge the Defence Science and Technology Organisation for the loan of the 5 kHz pump source. This work was funded by an Australian Research Council Discovery Grant. R. Mildren's e-mail address is rmildren@ics.mq.edu.au.

References

1. D. W. Coutts and A. J. S. McGonigle, IEEE J. Quantum Electron. **40**, 1430 (2004).
2. See, for example J. Hecht, Laser Focus World **41**(22), 95 (2005).
3. H. M. Pask, Prog. Quantum Electron. **27**, 3 (2003).
4. C. He and T. H. Chyba, Opt. Commun. **135**, 273 (1997).
5. Y. F. Chen, Opt. Lett. **29**, 2172 (2004).
6. R. P. Mildren, H. M. Pask, H. Ogilvy, and J. A. Piper, Opt. Lett. **30**, 1500 (2005).
7. R. P. Mildren, M. Convery, H. M. Pask, J. A. Piper, and T. Mckay, Opt. Express **12**, 785 (2004).
8. P. Cerny and H. Jelinkova, Opt. Lett. **27**, 360 (2002).
9. R. P. Mildren, H. M. Pask, J. A. Piper, and T. McKay, in *Conference Digest European Conference on Lasers and Electro-Optics* (European Physical Society, 2005), paper CA-38-Mon.
10. V. V. Ermolenkov, V. A. Lisinetskii, Ya. I. Mishkel, A. S. Grabchikov, A. P. Chaikovskii, and V. A. Orlovich, J. Opt. Technol. **72**, 32 (2005).
11. J. Richards and A. McInnes, Opt. Lett. **20** 37l (1995).